

Article

The Role of Acetate Kinase in the Human Parasite *Entamoeba histolytica*

Thanh Dang ^{1,2,†}, Matthew Angel ^{1,2,†}, Jin Cho ^{1,2}, Diana Nguyen ^{1,2} and Cheryl Ingram-Smith ^{1,2,*}

¹ Department of Genetics and Biochemistry, Clemson University, Clemson, SC 29634, USA; thanhhd@g.clemson.edu (T.D.); mbangel@g.clemson.edu (M.A.); jinc@g.clemson.edu (J.C.); nguyendiana@outlook.com (D.N.)

² Eukaryotic Pathogens Innovation Center, Clemson University, Clemson, SC 29634, USA

* Correspondence: cheryli@clemson.edu; Tel.: +1-864-656-2376

† These authors contributed equally to this work.

Abstract: The human parasite *Entamoeba histolytica*, which causes approximately 100 million cases of amoebic dysentery each year, relies on glycolysis as the major source of ATP production from glucose as it lacks a citric acid cycle and oxidative phosphorylation. Ethanol and acetate, the two major glycolytic end products for *E. histolytica*, are produced at a ratio of 2:1 under anaerobic conditions, creating an imbalance between NADH production and utilization. In this study we investigated the role of acetate kinase (ACK) in acetate production during glycolysis in *E. histolytica* metabolism. Analysis of intracellular and extracellular metabolites demonstrated that acetate levels were unaffected in an ACK RNAi cell line, but acetyl-CoA levels and the NAD⁺/NADH ratio were significantly elevated. Moreover, we demonstrated that glyceraldehyde 3-phosphate dehydrogenase catalyzes the ACK-dependent conversion of acetaldehyde to acetyl phosphate in *E. histolytica*. We propose that ACK is not a major contributor to acetate production, but instead provides a mechanism for maintaining the NAD⁺/NADH balance during ethanol production in the extended glycolytic pathway.



Citation: Dang, T.; Angel, M.; Cho, J.; Nguyen, D.; Ingram-Smith, C. The Role of Acetate Kinase in the Human Parasite *Entamoeba histolytica*. *Parasitologia* **2022**, *2*, 147–159. <https://doi.org/10.3390/parasitologia2020014>

Academic Editor: Geoff Hide

Received: 11 May 2022

Accepted: 13 June 2022

Published: 16 June 2022

Publisher's Note: MDPI stays neutral with regard to jurisdictional claims in published maps and institutional affiliations.



Copyright: © 2022 by the authors. Licensee MDPI, Basel, Switzerland. This article is an open access article distributed under the terms and conditions of the Creative Commons Attribution (CC BY) license (<https://creativecommons.org/licenses/by/4.0/>).

Keywords: *Entamoeba histolytica*; acetate kinase; glycolysis

1. Introduction

Entamoeba histolytica is an amoebic parasite that causes diarrheal illness in an estimated 100 million people worldwide [1] as well as amoebic liver abscess that results in 50,000–100,000 deaths annually [2]. Infection proceeds through an oral–fecal route, resulting in *E. histolytica* colonization within the large intestine [3,4]. This amitochondriate parasite lacks many essential biosynthetic pathways including the citric acid cycle and oxidative phosphorylation, and glycolysis is the primary pathway for ATP generation during growth on glucose [5,6]. Unlike the standard glycolytic pathway, *E. histolytica* glycolysis is pyrophosphate (PP_i)-dependent. Instead of ATP-dependent phosphofructokinase and pyruvate kinase, *E. histolytica* possesses PP_i-dependent phosphofructokinase and pyruvate phosphate dikinase [7–10]. Pyrophosphate, therefore, plays an important role in energy conservation.

Ultimately, *E. histolytica* produces ethanol and acetate as the major end products during growth on glucose [11,12]. Ethanol is produced by the bifunctional alcohol/aldehyde dehydrogenase ADHE in a two-step pathway (Figure 1) [13–15]. *E. histolytica* has two potential acetate-producing enzymes, acetate kinase (ACK) [16,17] and ADP-forming acetyl-CoA synthetase (ACD) (Figure 1) [12,18]. ACK (EC 2.3.1.8) is a phosphotransferase that interconverts acetyl phosphate and acetate. It is widespread in bacteria where it primarily functions in a pathway with phosphotransacetylase (PTA; EC 2.3.1.8) to activate acetate to acetyl-CoA or produce acetate and ATP from acetyl-CoA [19]. In the archaeal genus *Methanosarcina* ACK forms a pathway with PTA for the activation of acetate as a substrate for methane production [20,21]. ACK, previously thought to be absent in eukaryotes, has

now been identified in eucaryote and basidiomycete fungi in which it forms with xylulose 5-phosphate/fructose 6-phosphate phosphoketolase (XFP; EC 4.1.2.22) for the production of acetate [22]. ACK partners with PTA in the green alga *Chlamydomonas reinhardtii* [23] and the oomycete *Phytophthora* [22].

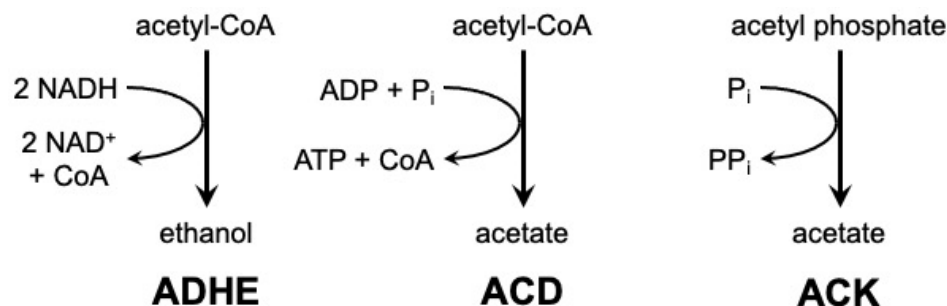


Figure 1. Ethanol and acetate production in *E. histolytica*. ADHE (left) catalyzes production of ethanol from acetyl-CoA. ACD (middle) and ACK (right) produce acetate from acetyl-CoA and acetyl phosphate, respectively.

ACK has also been identified in *Entamoeba* and characterization of the recombinant *E. histolytica* ACK (EhACK) revealed it to be phosphate/pyrophosphate (P_i/PP_i)-dependent, a stark contrast to all other characterized ACKs which are ATP/ADP-dependent [16,17]. EhACK operates primarily in the acetate/PP_i-producing direction in vitro [16,17]. Consistent with this, activity was detected only in the acetate/PP_i-producing direction in cell extract [16,17], supporting this as the physiological direction of EhACK. However, the role of ACK in *E. histolytica* still remains undefined and a partner enzyme that produces the acetyl phosphate substrate has not yet been identified. Harting and Velick [24,25] demonstrated that rabbit muscle glyceraldehyde 3-phosphate dehydrogenase (GAPDH) can produce acetyl phosphate from acetaldehyde, raising this as a possible new partner for ACK.

Here, we investigated the physiological role of ACK in *E. histolytica* and evaluated whether EhACK is the primary enzyme responsible for acetate production during growth on glucose. Growth of an ACK RNAi cell line was unaffected versus the wild-type and a control RNAi cell line and extracellular acetate and ethanol levels were comparable between the three cell lines. Intracellular ATP levels were also unaffected, but the ACK RNAi cell line had higher intracellular acetyl-CoA and an increased NAD⁺/NADH ratio. We demonstrated that recombinant *E. histolytica* GAPDH (EhGAPDH) can use acetaldehyde as a substrate, but only in the presence of ACK. Based on this evidence, we propose that EhACK functions to maintain the proper NAD⁺/NADH balance for ethanol production during glycolysis and is not a major contributor to acetate production.

2. Results

2.1. Trigger-Mediated ACK Gene Silencing

To investigate the role of ACK in *E. histolytica*, we created an ACK RNAi cell line to examine the effect of ACK gene silencing on growth and metabolism. The EhACK gene was silenced using the trigger-mediated small antisense gene silencing method developed by Morf et al. [26]. The pKT3M vector used for this has a resident luciferase gene (*LUC*) and is used as a control. The EhACK coding sequence was cloned into the pKT3M vector to replace the resident luciferase gene (*LUC*) and transfected into wild-type *E. histolytica*. A *LUC* RNAi cell line was also constructed to be used as a control cell line that would be under the same G418 selection as the ACK RNAi cell line. RT-PCR was performed to examine ACK transcript levels in wild-type, the control *LUC* RNAi cell line, and the ACK RNAi cell line. ACK mRNA levels were comparable in the wild-type and the *LUC* RNAi cell line but undetectable in the ACK RNAi cell line (Figure 2a). Enzymatic assays demonstrated that ACK enzymatic activity was reduced 18-fold in the ACK RNAi cell line

but was unaffected in the control *LUC* RNAi cell line (Figure 2b). Taken together, these results confirmed successful *ACK* silencing in the *ACK* RNAi cell line.

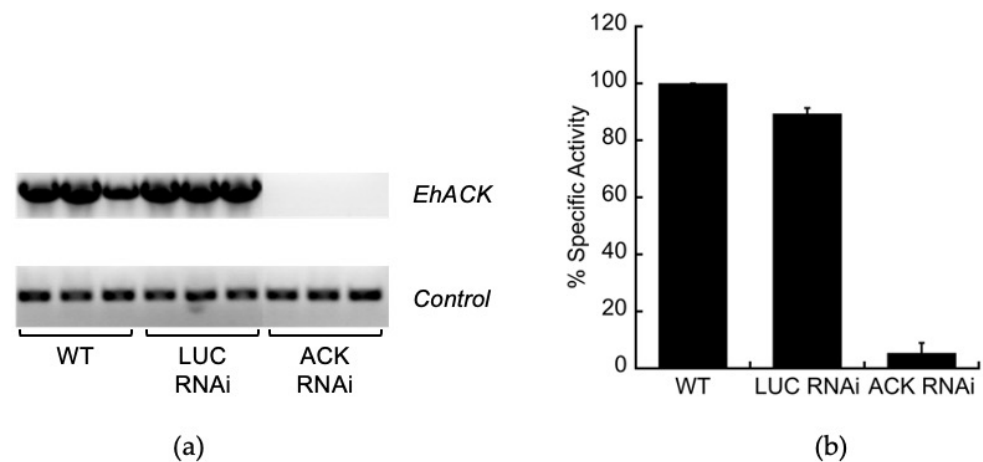


Figure 2. *ACK* expression and activity in the *EhACK* RNAi cell line. (a) Expression of *EhACK* in the wild-type (WT), control *LUC* RNAi, and *EhACK* RNAi cell lines was examined by RT-PCR (top). Expression of a constitutive control gene encoding a small ribosomal subunit was used as a loading control (bottom). Each RT-PCR reaction was performed in triplicate. (b) *ACK* activity in the acetate-forming direction was measured using the reverse hydroxamate assay. Activities are the mean \pm standard deviation of three replicates. All specific activities are normalized to that observed for extracts from the wild-type, represented as 100%.

2.2. *ACK* Is Dispensable for Growth on Glucose

One potential role for *ACK* is in acetate production in an extended glycolytic pathway. Acetate and ethanol are the main end products during *E. histolytica* growth on glucose [11,12] and we hypothesized that if *ACK* plays a primary role in acetate production, then an *ACK* RNAi cell line would have impaired growth on glucose. We measured growth in standard TYI-S-33 medium, which contains 50 mM added glucose (designated here as TYI glucose), and in TYI-S-33 medium in which the added glucose has been lowered to 10 mM (designated here as TYI low glucose). Growth of the wild-type, *LUC* RNAi, and *ACK* RNAi cell lines was similar at both glucose levels (Figure 3).

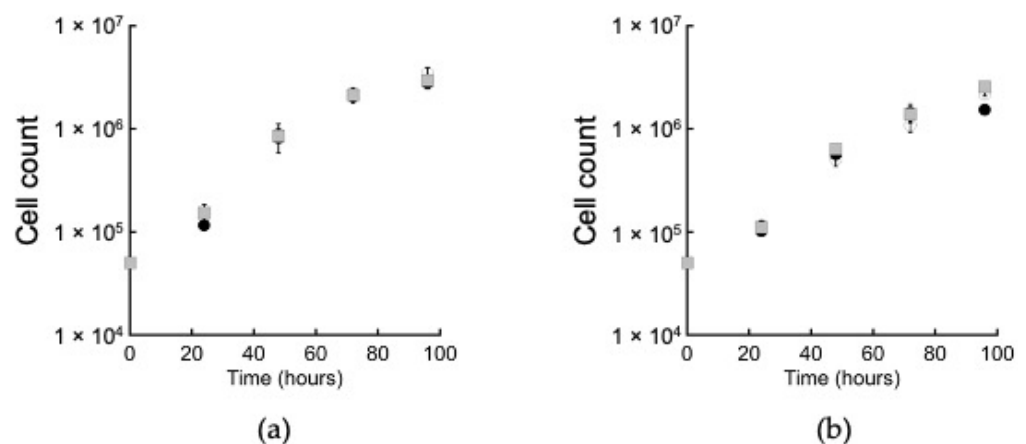


Figure 3. Growth of the *ACK* RNAi cell line in (a) TYI glucose medium, and (b) TYI low glucose medium. Open circles (\circ), wild-type; closed circles (\bullet), *LUC* RNAi cell line; gray squares (\blacksquare), *EhACK* RNAi cell line. Cell counts are the mean \pm standard deviation of three biological replicates.

2.3. Intracellular but Not Extracellular Metabolite Levels Are Altered in the *ACK* RNAi Cell Line

To evaluate *EhACK*'s role in glycolysis, we determined intracellular acetyl-CoA and ATP levels in cells grown 48 h in TYI glucose medium as measures of glycolytic activity and

intracellular energy levels. The *ACK* RNAi cell line showed an accumulation of acetyl-CoA, with a level ~172% that of the wild-type and the *LUC* RNAi cell line, but the intracellular ATP level was unaffected (Figure 4a). The *ACK* RNAi cell line also experienced ~2.5-fold increased NAD^+/NADH ratio versus that observed for the *LUC* RNAi cell line and ~4.9-fold higher than for the wild-type cell line (Figure 4b). Intracellular NADH was reduced in the both the *LUC* RNAi and *ACK* RNAi cell lines to $56.3 \pm 25.0\%$ and $21.9 \pm 0.3\%$ that of the wild-type, respectively. One possible explanation for why the *LUC* RNAi cell line had a higher NAD^+/NADH ratio than observed in the wild-type is that it is under G418 selection. However, the *ACK* RNAi cell line, also under G418 selection, still exhibited a significantly higher NAD^+/NADH ratio than the *LUC* cell line.

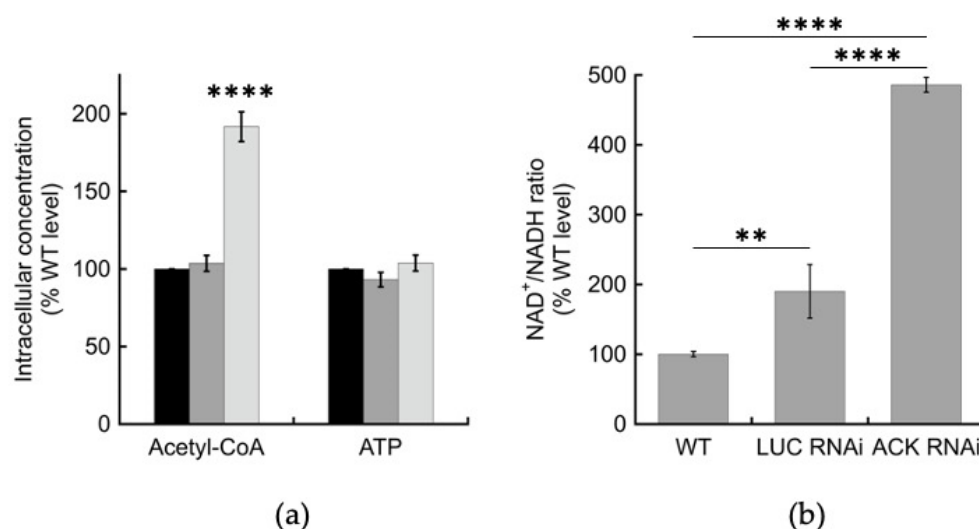


Figure 4. Intracellular metabolite levels in *ACK* RNAi cells. Metabolites were extracted using methanol extraction from log-phase trophozoites and concentrations were measured using LC-MS/MS. (a) Concentrations of acetyl-CoA and ATP. Wild-type (■), *LUC* RNAi (▣), *EhACK* RNAi cells (▨). (b) Ratio of NAD^+/NADH , normalized to wild-type ratio. Measurements are the mean \pm standard deviation of three to five replicates. ** p -value ≤ 0.01 ; **** p -value ≤ 0.0001 .

The ratio of extracellular ethanol to acetate produced by *E. histolytica* during growth on glucose varies depending on oxygen level [11,12]. To determine if *ACK* plays a significant role in the production of acetate and impacts the ethanol:acetate ratio, we measured extracellular acetate and ethanol in spent medium from the wild-type, *LUC* RNAi, and *ACK* RNAi cell lines grown for 48 h in TYI glucose medium (Figure 4). Production of acetate and ethanol was similar in the *ACK* RNAi cell line versus the wild-type cell line or the *LUC* RNAi control cell line (Figure 5). The calculated ratios of ethanol to acetate were found to be 1.8:1, 1.7:1, and 1.6:1 for the wild-type, *LUC* RNAi, and *ACK* RNAi cell lines, respectively.

2.4. *ACK* Does Not Play a Role in Utilization of Short Chain Fatty Acids

E. histolytica colonizes the human colon, where glucose is scarce as most dietary glucose is absorbed in the small intestine. Short chain fatty acids (SCFAs) are abundant though with a total concentration of 110–120 mM mainly consisting of acetate, propionate, and butyrate at a relative molar mass ratio of 57:22:21, respectively [27]. Although kinetic analysis showed *EhACK* strongly favors acetate production [16,28], we examined whether it plays a role in growth on SCFAs. Wild-type, *LUC* RNAi, and *ACK* RNAi cell lines were grown in TYI-S-33 medium lacking glucose (designated as TYI basal medium) or TYI basal medium supplemented with 63 mM acetate, 24 mM propionate, or 23 mM butyrate (final concentration) for 72 h. These concentrations represent the estimated concentrations found in the colon based on total SCFA abundance and relative molar ratios. Growth of the *ACK* RNAi cell line was similar to that of the wild-type and the *LUC* RNAi cell line for all four media (Figure 6). Interestingly, all three cell lines showed slightly enhanced growth in the

presence of added propionate versus TYI basal medium (p -value ≤ 0.01 for wild-type and *LUC* RNAi cell lines; p -value ≤ 0.001 for *ACK* RNAi cell line), but the presence of acetate or butyrate had no effect.

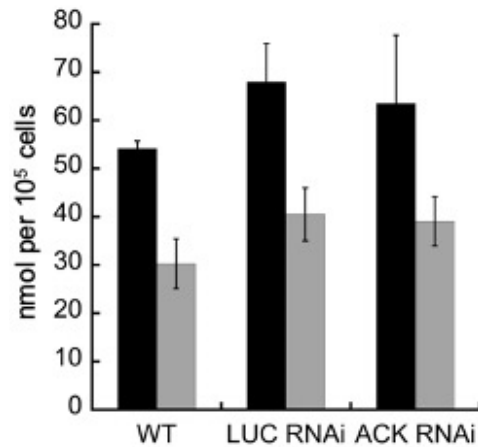


Figure 5. Extracellular ethanol and acetate levels in spent TYI glucose medium. Ethanol (■) and acetate (■) were measured in spent medium from cultures of wild-type, *LUC* RNAi, and *ACK* RNAi cell lines grown in TYI glucose medium for 48 h. The results shown represent the mean \pm standard deviation for four to five biological replicates for each cell line. Unpaired *t*-test revealed no statistical difference between cell lines for either ethanol or acetate.

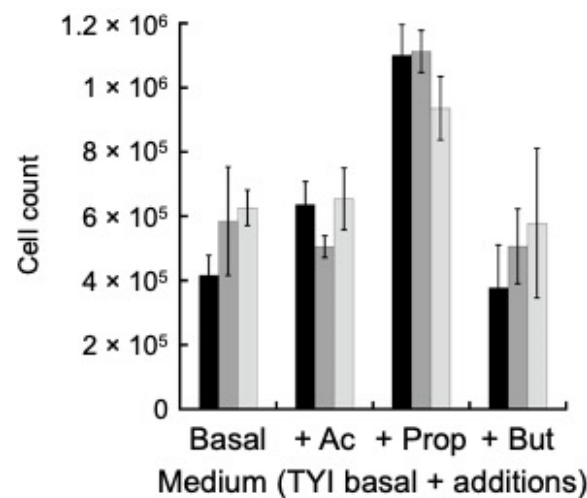


Figure 6. Growth of *EhACK* RNAi cells in basal medium supplemented with short chain fatty acids (SCFAs). Cells were grown for 72 h in TYI basal medium or TYI basal medium supplemented with acetate (Ac), propionate (Prop), or butyrate (But). Wild-type (■), *LUC* RNAi (■), *EhACK* RNAi cells (□). Cell counts are the mean \pm standard deviation of three biological replicates.

2.5. Oxidative and Nitrosative Stress Response Are Unaffected in the *ACK* RNAi Cell Line

We examined the effect of oxidative stress on an *ACK* RNAi cell line by exposing log-phase trophozoites to oxidative stress from exposure to hydrogen peroxide. Cells were grown in TYI glucose or TYI basal medium, exposed to 5 mM hydrogen peroxide (final concentration) for 3 h, and the change in viability was measured. The *ACK* RNAi cell line displayed similar changes in viability due to oxidative stress as the wild-type and *LUC* RNAi control cell lines (Figure 7a). When grown on TYI glucose medium, all three cell lines exhibited greater than 50% reduced viability after hydrogen peroxide exposure versus mock treated control cells. When grown on TYI basal medium though, the cell lines exhibited only ~20% reduced viability after hydrogen peroxide exposure versus mock treated control cells (Figure 7a).

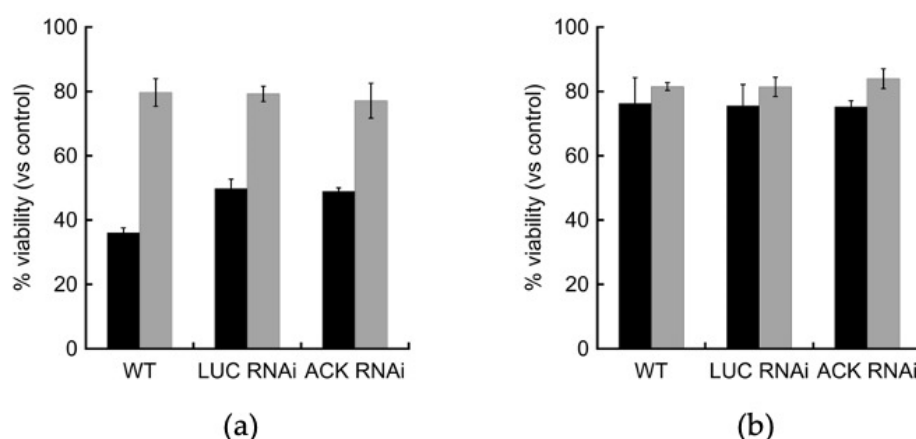


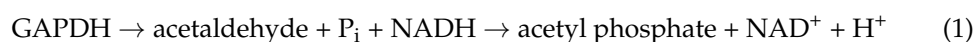
Figure 7. Effects of oxidative and nitrosative stress on *ACK* RNAi cells. Log-phase trophozoites in liquid medium were exposed to (a) 5 mM hydrogen peroxide (final concentration) for three hours at 37 °C to examine the effects of oxidative stress or to (b) 5 mM sodium nitroprusside (final concentration) for three hours at 37 °C to examine the effects of nitrosative stress. Viability for TYI glucose-grown (■) and TYI basal-grown (▒) cells was determined using trypan blue exclusion. Values shown are the mean ± SD of three biological replicates. Unpaired *t*-test showed statistically significant difference in viability reduction in response to oxidative stress when grown on TYI glucose medium compared to growth on TYI basal medium.

To examine the effect of nitrosative stress on *ACK* RNAi cells, we exposed trophozoites grown in TYI glucose and TYI basal medium to 5 mM sodium nitroprusside (final concentration) for three hours at 37 °C to examine the effects of nitrosative stress on cell viability. The effect was similar for all three cell lines, which exhibited ~24% decreased viability versus mock treated cells when grown on TYI glucose medium and 16–18% reduced viability when grown in TYI basal medium (Figure 7b).

2.6. *EhGAPDH* Displays Acetyl Phosphate-Forming Activity in the Presence of *ACK*

Although *ACK* activity has been detected in *E. histolytica* cell extracts [16], the source of the acetyl phosphate substrate has remained unknown as the typical partner enzymes PTA and XFP are absent in *E. histolytica*. In 1954, Harting and Velick demonstrated that rabbit muscle and yeast glyceraldehyde 3-phosphate dehydrogenase (*GAPDH*) can catalyze the phosphorylation of acetaldehyde to form acetyl phosphate [24,25]. This enzyme is typically used to catalyze the phosphorylation of glyceraldehyde 3-phosphate to 1,3-bisphosphoglycerate in an NAD⁺-dependent reaction as part of glycolysis, and *E. histolytica* has three nearly identical genes encoding *GAPDH*.

We have purified recombinant *EhGAPDH* and demonstrated NADH-dependent activity with glyceraldehyde 3-phosphate (Jin Cho, personal communication). We also tested activity with acetaldehyde as a substrate (reaction 1), but no activity was detectable, despite varying the reaction conditions, substrate concentrations, and amount of enzyme (Jin Cho, personal communication). We next tested *GAPDH* activity with acetaldehyde in the presence of purified recombinant *ACK* as this coupling might draw the reaction in the direction of acetyl phosphate production. We used the purified recombinant enzymes *EhACK* (reaction 2a) [16,28] and the well-characterized *Methanosarcina thermophila* *ACK* (*MtACK*; reaction 2b) [29–32] for these coupled reactions. The coupled *GAPDH-ACK* reactions would be expected to proceed as follows:



We measured GAPDH activity by following conversion of NADH to NAD⁺ with acetaldehyde as substrate. As shown in Table 1, GAPDH activity with acetaldehyde was observed only in the presence, but not absence, of ACK. To confirm that GAPDH's use of acetaldehyde as a substrate is dependent on ACK enzymatic activity, we used both EhACK and MtACK as the coupling enzyme in the presence and absence of ADP (P_i is already present in the reaction as a substrate for GAPDH (Equation (1)). EhACK is P_i-dependent (Equation (2a)) and the presence of ADP would not be expected to enhance GAPDH activity. As expected, the presence of ADP did not enhance GAPDH activity with EhACK as the coupling enzyme and instead inhibited activity, most likely because ADP acts as an inhibitor of EhACK [28]. MtACK's activity is ADP-dependent (Equation (2b)) and we, thus, expected increased GAPDH activity in the presence of ADP. Indeed, GAPDH activity increased 50-fold in the presence versus absence of ADP when MtACK was used as the coupling enzyme. Thus, our results indicate that GAPDH activity with acetaldehyde is ACK-dependent and requires the appropriate phosphoryl donor for the ACK partner enzyme.

Table 1. GAPDH activity with acetaldehyde in the presence and absence of ACK.

Enzymes	Specific Activity (nmol min ⁻¹ mg ⁻¹) ¹	
	No ADP	10 mM ADP
GAPDH	ND	ND
GAPDH + EhACK	14.1 ± 0.60	7.04 ± 0.90
GAPDH + MtACK	2.29 ± 0.16	128 ± 2.33

¹ All assays were performed in the presence of 2.5 mM P_i. ND—not detected.

3. Discussion

EhACK has been hypothesized to provide supplemental pyrophosphate for the pyrophosphate-dependent glycolytic pathway in *E. histolytica*. In a comparison between the transcriptome of the virulent HM-1:IMSS and the nonvirulent Rahman cell lines, several glycolytic enzymes including PP_i-PFK were found to be highly upregulated in HM-1:IMSS in both axenic culture and during contact with human colon explant [33]. This upregulation was thought to reflect the carbon metabolism needs during colonic mucosa degradation and tissue destruction during intestinal amoebiasis. EhACK is constitutively expressed in active trophozoites and at a slightly higher level in HM-1:IMSS versus the Rahman cell line [33–35]. These findings supported the possibility that EhACK could work in unison with PP_i-PFK and PPDK to drive glycolysis, although the source of the acetyl phosphate substrate for ACK was unknown.

Here, we used RNAi gene silencing to investigate the role of ACK in *E. histolytica* metabolism. As acetate and ethanol are the two primary end products of glucose breakdown, we hypothesized that if ACK's primary role is production PP_i for glycolysis, then growth on glucose would be affected in an ACK RNAi cell line. This was not the case though, as growth in low and high glucose media was similar for the ACK RNAi cell line and the control LUC RNAi and wild-type cell lines. Measurements of extracellular acetate and ethanol, the primary products of glucose metabolism in *E. histolytica* [11,12], revealed no difference between the three cell lines either. These results suggest that ACK is not a major contributor to acetate production, and thus not PP_i production either, at least not during standard growth on glucose as the main carbon and energy source. Pineda et al. similarly found that acetate and ethanol production were unaffected in an ACK RNAi cell line of the *E. histolytica* HM-1:IMSS G3 clone [36].

Acetate and ethanol are produced as part of an extended glycolytic pathway in which pyruvate is first converted to acetyl-CoA, which is then broken down to acetate and ethanol by ADP-forming acetyl-CoA synthetase (ACD) and alcohol dehydrogenase (ADHE), respectively (Figure 8). Ethanol production by ADHE is a two-step reaction with acetaldehyde as an intermediate [10]. Each step requires one NADH for a total of two NADH per pyruvate converted to ethanol, yet glycolysis only generates one NADH molecule per pyruvate

produced leading to an imbalance. Shunting pyruvate toward acetate production by ACD would help relieve this imbalance though as NADH is not required for this reaction. A 1:1 ratio of ethanol to acetate production would fully balance NADH production by glycolysis with NADH consumption by ADHE. However, we observed a ratio closer to 2:1 ethanol:acetate, similar to previously published values [11], suggesting an imbalance would be present.

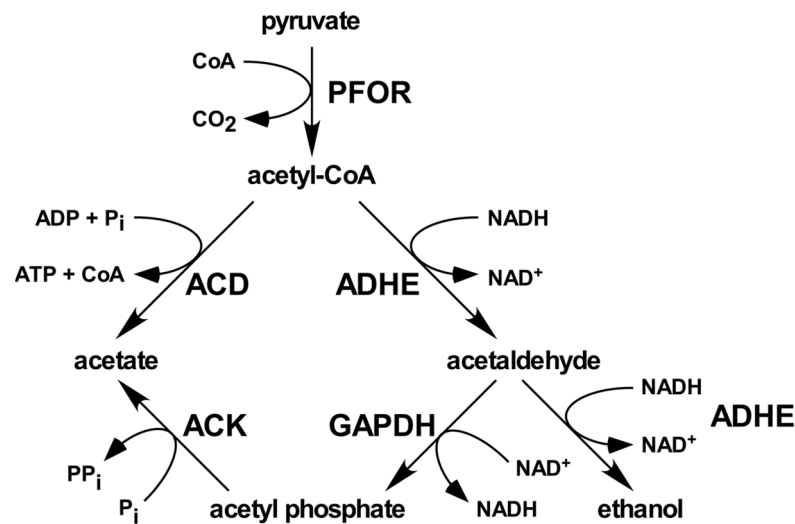


Figure 8. The extended glycolytic pathway in *E. histolytica* and the proposed role for ACK and GAPDH. Abbreviations are as follows: PFOR: pyruvate:ferredoxin oxidoreductase; ADHE: alcohol/aldehyde dehydrogenase; GAPDH: glyceraldehyde 3-phosphate dehydrogenase; ACK: acetate kinase; ACD: acetyl-CoA synthetase (ADP-forming).

We propose that EhACK plays a role in the extended glycolytic pathway in maintaining the proper NAD^+/NADH ratio during growth on glucose. In this proposed pathway, shown in Figure 8, when NADH levels are insufficient to continue ethanol production, acetaldehyde produced in the first step of the ADHE reaction would be released to GAPDH, which would then convert it to acetyl phosphate for use by ACK. NADH would be generated in this process to restore balance and allow ethanol production to continue. This would be expected to be an overflow pathway that would not be a major contributor to acetate production but would help maintain proper balance between the acetate and ethanol production.

Consistent with this proposed pathway, we showed that GAPDH can indeed use acetaldehyde as a substrate, but only when ACK was present to draw the reaction toward acetyl phosphate production. We observed that an ACK RNAi cell line has increased intracellular acetyl-CoA, suggesting that the inability to shunt acetaldehyde into a GAPDH-ACK pathway causes a slowdown of the ADHE pathway. Pineda et al. were unable to detect intracellular acetyl phosphate in *E. histolytica* grown in TYI glucose medium [36], but this is consistent with the proposed pathway in which the acetyl phosphate would be quickly converted to acetate by ACK.

We induced oxidative and nitrosative stress in *E. histolytica* trophozoites to observe the effect that reduced ACK activity would have on cell viability under variable glucose conditions. We observed that induction of oxidative stress had a more negative effect on viability in the presence of glucose versus the absence of glucose for all three cell lines, suggesting that *E. histolytica* tolerates oxidative stress better when glycolysis is less active. Reduction in ACK activity in the ACK RNAi cell line did not confer an advantage or disadvantage for oxidative stress tolerance. Given that ACK does not seem to be a major contributor to PP_i production and cell growth, this result was not unexpected. Our data are consistent with previous research that showed ACK was not significantly differentially expressed in cells exposed to oxidative stress [37]. Likewise, reduction in ACK activity did

not confer an advantage or disadvantage for nitrosative stress tolerance either; however, *ACK* RNAi cells tolerated nitrosative stress better in the absence of glucose than in glucose-containing medium. The reason for this is not known.

Finally, we examined whether acetate, propionate, or butyrate affected growth of *E. histolytica* in the absence of glucose. Growth increased when propionate, but not acetate or butyrate, was present. That *ACK* gene silencing did not influence increased growth with propionate is not surprising, as the EhACK reaction proceeds strongly in the direction of acetate/propionate production rather than utilization [16,17].

4. Materials and Methods

4.1. Chemicals and Reagents

Chemicals were purchased from Qiagen (Valencia, CA, USA) Promega (Madison, WI, USA), Sigma-Aldrich (St. Louis, MO, USA), VWR International (Radnor, PA, USA), Gold Biotechnology (Olivette, MO, USA), Fisher Scientific (Waltham, MA, USA), EMD Millipore (Burlington, MA, USA), and Life Technologies (Carlsbad, CA, USA). Penicillin-streptomycin solution and Diamond vitamins were purchased from Life Technologies (Carlsbad, CA, USA) and heat-inactivated adult bovine serum from GeminiBio (Sacramento, CA, USA). Restriction enzymes were purchased from New England Biolabs (Ipswich, MA, USA). Primers were purchased from Integrated DNA Technologies (Coralville, IA, USA).

4.2. Cell Lines and Culture Conditions

E. histolytica HM-1:IMSS was grown axenically at 37 °C in Diamond's TYI-S-33 medium [38] (17.95 g tryptone, 9.66 g yeast extract, 9.2 g glucose, 1.84 g NaCl, 0.92 g K₂HPO₄, 1.15 g cysteine, 0.178 g ascorbic acid, 0.0194 g ammonium ferric chloride, 15% *v/v* adult bovine serum, 1.73% *v/v* penicillin-streptomycin, and 2.62% *v/v* Diamond vitamins per liter, final pH 6.8). Trophozoites in log phase growth were used for all experiments. Modifications to media formulations and their designations are as follows: TYI glucose, standard TYI-S-33 medium (which contains 50 mM added glucose as shown above); TYI basal, TYI-S-33 medium without added glucose; and TYI low glucose, TYI-S-33 medium with the added glucose reduced to 10 mM. Growth on acetate, propionate, or butyrate was performed in TYI basal medium supplemented with 63 mM acetate (TYI acetate), 24 mM propionate (TYI propionate), or 23 mM butyrate (TYI butyrate). These concentrations of short chain fatty acids represent those found in the large intestine [27].

Growth curves were determined by counting cells every 24 h using a Luna Automated counter (Logos Biosystem, Annandale, VA, USA). Trypan blue exclusion was used to distinguish viable from dead cells [39]. Growth curves were performed with three biological replicates and values for each time point represent the mean ± standard deviation.

4.3. Construct Cloning and Transfection

The plasmid pKT3M (kindly provided by Dr. Upinder Singh, Stanford University, Stanford, CA, USA) [26] was used for construction of an *ACK* RNAi cell line. The full-length *Entamoeba histolytica* *ACK* coding sequence (EHI_170010) was PCR-amplified from *E. histolytica* genomic DNA using KOD Hot Start Polymerase (EMD Millipore, Billerica, MA, USA). The PCR product was cloned into *AvrII* and *XhoI* restriction sites to replace the resident luciferase (*LUC*) control gene. The final construct was confirmed by sequencing.

E. histolytica trophozoites were transfected with the *ACK* RNAi construct or the control pKT3M plasmid by electroporation as described previously [40,41]. A total of 2.4×10^6 cells were electroporated with 100 µg of DNA using two consecutive pulses at 1.2 kV and 25 µF and inoculated into TYI-S-33 medium. Transfectants were selected after two days by adding G418 to the medium to a final concentration of 6 µg/mL. Stable transfectants were maintained under this level of G418 selection. Primers used for construction of the *ACK* RNAi plasmid are listed Table 2.

Table 2. Primers for RNAi construct generation and RT-PCR confirmation.

Cloning Primers	
<i>EhACK</i> RNAi F	5' CTACCTAGGATGTCTAACGTACTAATATTCAACG
<i>EhACK</i> RNAi R	5' CTACTCGAGTTAAAAGTAAATAATTCTTTTCCTTTTGTAA
RT-PCR primers	
<i>EhACK</i> RTPCR F	5' AGGGTAAATGTTACAGGAACAGA
<i>EhACK</i> RTPCR R	5' TGGTGCCACACAAACTTGAAC
ssrRNA F	5'-AGGCGCGTAAATTACCCACTTTCG
ssrRNA R	5'-CACCAGACTTGCCCTCCAATTGAT

4.4. Reverse Transcriptase PCR (RT-PCR)

RT-PCR primers are listed in Table 2. RNA was isolated from 2×10^6 trophozoites using the RNeasy mini kit (Qiagen, Valencia, CA, USA) or Trizol reagent according to the manufacturers' instructions. RT-PCR was employed to determine whether the *EhACK* gene was silenced in the *ACK* RNAi cell line. RT-PCR was performed using the One-Step RT-PCR kit (Qiagen) using 30 cycles. RNA levels were normalized for comparison using the small subunit ribosomal RNA gene (accession number: X61116) as previously described [42].

4.5. Enzyme Assays

EhACK knockdown was confirmed by measuring *ACK* activity in cell lysates. A total of 4×10^6 cells were harvested by centrifugation and washed twice in phosphate buffered saline (PBS). Cells were resuspended in 25 mM Tris, 150 mM NaCl (pH 7.4) and lysed by vortexing with acid-washed beads for 1 min, followed by 1 min on ice. This cycle was repeated three times. The lysates were centrifuged at $5000 \times g$ for 15 min and the supernatant was retained.

ACK activity was measured using the reverse hydroxamate assay as previously described [16]. Enzyme activity was assessed in a 300 μ L reaction containing 50 mM sodium phosphate, 2 mM acetyl phosphate, 100 mM Tris-HCl (pH 7.0), 10 mM $MgCl_2$, and 50 μ L cell lysate at 37 °C. Reactions were terminated after 30 min by adding 100 μ L of the development solution (0.92 M trichloroacetic acid, 250 mM $FeCl_3$, and 2.5 N HCl). Absorbance at 540 nm was measured using a Synergy Epoch microplate reader (Biotek, Winooski, VT, USA).

GAPDH activity with acetaldehyde as substrate was determined using a spectrophotometric assay that measures the conversion of NAD^+ to NADH. The reaction mix contained 25 mM Tris-HCl (pH 7.0), 2.5 mM potassium phosphate buffer (pH 7.0), 1 mM NAD^+ , and 1 mM DTT. Reactions were performed in the presence or absence of recombinant *E. histolytica* *ACK* (*EhACK*) [16] or *Methanosarcina thermophila* *ACK* (*MtACK*) [29,30] as a coupling enzyme to convert acetyl phosphate to acetate to draw the reaction forward. The reaction was initiated by addition of acetaldehyde to a final concentration of 500 mM and the absorbance change at 340 nm was measured to monitor the conversion of NAD^+ to NADH at 37 °C using a Synergy Epoch microplate reader (Biotek, Winooski, VT, USA).

Total protein concentration in cell lysates was measured using the Bradford assay [43,44] with bovine serum albumin as the standard.

4.6. Intracellular Metabolite Analysis

E. histolytica intracellular metabolites were extracted using an adapted methanol extraction method [45] from 1×10^6 log phase trophozoites. Cells were harvested by centrifugation, washed three times in ice cold 5% mannitol solution, and resuspended in 1.5 mL ice cold 100% methanol. Trophozoites were lysed using three freeze-thaw cycles in which cells were frozen in liquid nitrogen for 5 min and thawed on dry ice for 10 min. The lysate was centrifuged at $10,000 \times g$ for 5 min and the supernatant isolated. Samples were analyzed at the Clemson Multi-User Analytic Lab via LC-MS/MS. Intracellular metabolite concentrations were calculated by assuming *E. histolytica* trophozoites have an intracellular volume of 1.3 μ L per 1×10^6 cells as previously reported [45].

4.7. Extracellular Metabolite Analysis

Acetate in spent TYI glucose medium from 48 h cultures was measured using the hydroxamate assay in which acetate is converted to acetyl phosphate, which is then converted to an acetyl hydroxamate complex that can be detected spectrophotometrically [46]. Reactions (300 μ L) contained 150 μ L reaction mix [100 mM Tris-HCL (pH 7.0), 600 mM hydroxylamine HCl (pH 7.0), 10 mM MgCl₂, 10 mM ATP, 100 μ g recombinant MtACK], and 150 μ L spent medium. Reactions were incubated at 37 °C and terminated after 30 min by adding 600 μ L of development solution (0.92 M trichloroacetic acid, 250 mM FeCl₃, and 2 N HCl). Samples were centrifuged at 10,000 \times g for 5 min to pellet precipitated proteins. The absorbance at 540 nM was measured using a Synergy Epoch microplate reader (Biotek, Winooski, VT, USA) and compared against a standard curve generated with acetyl phosphate.

Ethanol in spent TYI glucose medium from 48-h cultures was measured using the EnzyChrom™ Ethanol Assay Kit (BioAssay Systems, Hayward, CA, USA), which is based on the alcohol dehydrogenase-catalyzed oxidation of ethanol. Reactions were prepared according to the manufacturer's instructions and terminated after 30 min. Absorbance at 565 nM was measured using a Synergy Epoch microplate reader (Biotek, Winooski, VT, USA).

4.8. Oxidative Stress and Nitrosative Stress Induction

The effect of oxidative or nitrosative stress on *E. histolytica* trophozoites was determined by exposing trophozoites to hydrogen peroxide or sodium nitroprusside in liquid culture and then assessing change in cell viability. Log-phase trophozoites were harvested and counted using trypan blue exclusion [39] on a Luna Automated Counter (Logos Biosystem, Annandale, VA, USA). Samples containing 3.5×10^4 live cells resuspended in fresh, prewarmed TYI glucose medium were prepared for each culture. For oxidative stress, hydrogen peroxide was added to final concentration of 5 mM to one sample and an equal volume of water was added to the control sample. For nitrosative stress, sodium nitroprusside was added to a final concentration of 5 mM to one sample and an equal volume of water was added to the control sample. Sample tubes were rotated for 3 h at 37 °C, and cell viability was determined using trypan blue exclusion. The difference in cell viability between each sample and its control was recorded to determine the effect of oxidative or nitrosative stress on each cell type. Three biological replicates were performed for each cell type.

5. Conclusions

Contrary to our starting hypothesis, we found that ACK is unlikely to be a major contributor to acetate production or the PP_i pool in *E. histolytica*. Instead, our results suggest that ACK plays a role in the extended glycolytic pathway in *E. histolytica* to provide a mechanism for maintaining proper NAD⁺/NADH balance during glycolysis and ethanol production and, as such, could potentially play a role in partitioning of acetyl-CoA between acetate and ethanol production. Such a function may be essential under some conditions but not others, but this remains to be investigated.

Author Contributions: Conceptualization, C.I.-S.; methodology, C.I.-S., T.D., M.A. and J.C.; formal analysis, C.I.-S., T.D. and M.A.; investigation, T.D., M.A., J.C. and D.N.; writing—original draft preparation, T.D., M.A. and C.I.-S.; writing—review and editing, C.I.-S. All authors have read and agreed to the published version of the manuscript.

Funding: This research was funded by the National Institutes of Health, grant number R15GM114759 to C.I.-S. and grant number P20GM109094 to Lesly Temesvari and Kerry Smith (C.I.-S. supported as target investigator).

Institutional Review Board Statement: Not applicable.

Informed Consent Statement: Not applicable.

Data Availability Statement: Data presented in this study are available within the article.

Acknowledgments: We thank Kerry Smith and Lesly Temesvari (Clemson University) for their thoughtful suggestions regarding this work. *E. histolytica* HM1:IMSS was kindly provided by Temesvari.

Conflicts of Interest: The authors declare no conflict of interest.

References

1. World Health Organization; Foodborne Disease Burden Epidemiology Reference Group. *WHO Estimates of the Global Burden of Foodborne Diseases*; World Health Organization: Geneva, Switzerland, 2015; p. 11, 254p.
2. Baxt, L.A.; Singh, U. New insights into *Entamoeba histolytica* pathogenesis. *Curr. Opin. Infect. Dis.* **2008**, *21*, 489–494. [[CrossRef](#)] [[PubMed](#)]
3. Haque, R.; Huston, C.D.; Hughes, M.; Houpt, E.; Petri, W.A., Jr. Amebiasis. *N. Engl. J. Med.* **2003**, *348*, 1565–1573. [[CrossRef](#)] [[PubMed](#)]
4. Stanley, S.L., Jr. Amoebiasis. *Lancet* **2003**, *361*, 1025–1034. [[CrossRef](#)]
5. Anderson, I.J.; Loftus, B.J. *Entamoeba histolytica*: Observations on metabolism based on the genome sequence. *Exp. Parasitol.* **2005**, *110*, 173–177. [[CrossRef](#)]
6. Clark, C.G.; Alsmark, U.C.; Tazreiter, M.; Saito-Nakano, Y.; Ali, V.; Marion, S.; Weber, C.; Mukherjee, C.; Bruchhaus, I.; Tannich, E.; et al. Structure and content of the *Entamoeba histolytica* genome. *Adv. Parasitol.* **2007**, *65*, 51–190.
7. Reeves, R.E.; Serrano, R.; South, D.J. 6-phosphofructokinase (pyrophosphate). Properties of the enzyme from *Entamoeba histolytica* and its reaction mechanism. *J. Biol. Chem.* **1976**, *251*, 2958–2962. [[CrossRef](#)]
8. Saavedra, E.; Encalada, R.; Pineda, E.; Jasso-Chavez, R.; Moreno-Sanchez, R. Glycolysis in *Entamoeba histolytica*. Biochemical characterization of recombinant glycolytic enzymes and flux control analysis. *FEBS J.* **2005**, *272*, 1767–1783. [[CrossRef](#)]
9. Saavedra-Lira, E.; Perez-Montfort, R. Energy production in *Entamoeba histolytica*: New perspectives in rational drug design. *Arch. Med. Res.* **1996**, *27*, 257–264.
10. Lo, H.S.; Reeves, R.E. Pyruvate-to-ethanol pathway in *Entamoeba histolytica*. *Biochem. J.* **1978**, *171*, 225–230. [[CrossRef](#)]
11. Montalvo, F.E.; Reeves, R.E.; Warren, L.G. Aerobic and anaerobic metabolism in *Entamoeba histolytica*. *Exp. Parasitol.* **1971**, *30*, 249–256. [[CrossRef](#)]
12. Reeves, R.E.; Warren, L.G.; Susskind, B.; Lo, H.S. An energy-conserving pyruvate-to-acetate pathway in *Entamoeba histolytica*. Pyruvate synthase and a new acetate thiokinase. *J. Biol. Chem.* **1977**, *252*, 726–731. [[CrossRef](#)]
13. Pineda, E.; Encalada, R.; Olivos-Garcia, A.; Nequiz, M.; Moreno-Sanchez, R.; Saavedra, E. The bifunctional aldehyde-alcohol dehydrogenase controls ethanol and acetate production in *Entamoeba histolytica* under aerobic conditions. *FEBS Lett.* **2013**, *587*, 178–184. [[CrossRef](#)] [[PubMed](#)]
14. Pineda, E.; Encalada, R.; Rodriguez-Zavala, J.S.; Olivos-Garcia, A.; Moreno-Sanchez, R.; Saavedra, E. Pyruvate:ferredoxin oxidoreductase and bifunctional aldehyde-alcohol dehydrogenase are essential for energy metabolism under oxidative stress in *Entamoeba histolytica*. *FEBS J.* **2010**, *277*, 3382–3395. [[CrossRef](#)] [[PubMed](#)]
15. Espinosa, A.; Yan, L.; Zhang, Z.; Foster, L.; Clark, D.; Li, E.; Stanley, S.L., Jr. The bifunctional *Entamoeba histolytica* alcohol dehydrogenase 2 (EhADH2) protein is necessary for amebic growth and survival and requires an intact C-terminal domain for both alcohol dehydrogenase and acetaldehyde dehydrogenase activity. *J. Biol. Chem.* **2001**, *276*, 20136–20143. [[CrossRef](#)]
16. Fowler, M.L.; Ingram-Smith, C.; Smith, K.S. Novel pyrophosphate-forming acetate kinase from the protist *Entamoeba histolytica*. *Eukaryot. Cell* **2012**, *11*, 1249–1256. [[CrossRef](#)]
17. Reeves, R.E.; Guthrie, J.D. Acetate kinase (pyrophosphate). A fourth pyrophosphate-dependent kinase from *Entamoeba histolytica*. *Biochem. Biophys. Res. Commun.* **1975**, *66*, 1389–1395. [[CrossRef](#)]
18. Jones, C.P.; Ingram-Smith, C. Biochemical and kinetic characterization of the recombinant ADP-forming acetyl coenzyme A synthetase from the amitochondriate protozoan *Entamoeba histolytica*. *Eukaryot. Cell* **2014**, *13*, 1530–1537. [[CrossRef](#)]
19. Wolfe, A.J. The acetate switch. *Microbiol. Mol. Biol. Rev.* **2005**, *69*, 12–50. [[CrossRef](#)]
20. Terlesky, K.C.; Barber, M.J.; Aceti, D.J.; Ferry, J.G. EPR properties of the Ni-Fe-C center in an enzyme complex with carbon monoxide dehydrogenase activity from acetate-grown *Methanosarcina thermophila*. Evidence that acetyl-CoA is a physiological substrate. *J. Biol. Chem.* **1987**, *262*, 15392–15395. [[CrossRef](#)]
21. Singh-Wissmann, K.; Ferry, J.G. Transcriptional regulation of the phosphotransacetylase-encoding and acetate kinase-encoding genes (pta and ack) from *Methanosarcina thermophila*. *J. Bacteriol.* **1995**, *177*, 1699–1702. [[CrossRef](#)]
22. Ingram-Smith, C.; Martin, S.R.; Smith, K.S. Acetate kinase: Not just a bacterial enzyme. *Trends Microbiol.* **2006**, *14*, 249–253. [[CrossRef](#)] [[PubMed](#)]
23. Yang, W.; Catalanotti, C.; D’Adamo, S.; Wittkopp, T.M.; Ingram-Smith, C.J.; Mackinder, L.; Miller, T.E.; Heuberger, A.L.; Peers, G.; Smith, K.S.; et al. Alternative acetate production pathways in *Chlamydomonas reinhardtii* during dark anoxia and the dominant role of chloroplasts in fermentative acetate production. *Plant Cell* **2014**, *26*, 4499–4518. [[CrossRef](#)] [[PubMed](#)]
24. Harting, J.; Velick, S.F. Transfer reactions of acetyl phosphate catalyzed by glyceraldehyde-3-phosphate dehydrogenase. *J. Biol. Chem.* **1954**, *207*, 867–878. [[CrossRef](#)]
25. Harting, J.; Velick, S.F. Acetyl phosphate formation catalyzed by glyceraldehyde-3-phosphate dehydrogenase. *J. Biol. Chem.* **1954**, *207*, 857–865. [[CrossRef](#)]
26. Morf, L.; Pearson, R.J.; Wang, A.S.; Singh, U. Robust gene silencing mediated by antisense small RNAs in the pathogenic protist *Entamoeba histolytica*. *Nucleic Acids Res.* **2013**, *41*, 9424–9437. [[CrossRef](#)]
27. Cummings, J.H.; Pomare, E.W.; Branch, W.J.; Naylor, C.P.; Macfarlane, G.T. Short chain fatty acids in human large intestine, portal, hepatic and venous blood. *Gut* **1987**, *28*, 1221–1227. [[CrossRef](#)]

28. Dang, T.; Ingram-Smith, C. Investigation of pyrophosphate versus ATP substrate selection in the *Entamoeba histolytica* acetate kinase. *Sci. Rep.* **2017**, *7*, 5912. [[CrossRef](#)]
29. Aceti, D.J.; Ferry, J.G. Purification and characterization of acetate kinase from acetate-grown *Methanosarcina thermophila*. Evidence for regulation of synthesis. *J. Biol. Chem.* **1988**, *263*, 15444–15448. [[CrossRef](#)]
30. Latimer, M.T.; Ferry, J.G. Cloning, sequence analysis, and hyperexpression of the genes encoding phosphotransacetylase and acetate kinase from *Methanosarcina thermophila*. *J. Bacteriol.* **1993**, *175*, 6822–6829. [[CrossRef](#)]
31. Ingram-Smith, C.; Gorrell, A.; Lawrence, S.H.; Iyer, P.; Smith, K.; Ferry, J.G. Characterization of the acetate binding pocket in the *Methanosarcina thermophila* acetate kinase. *J. Bacteriol.* **2005**, *187*, 2386–2394. [[CrossRef](#)]
32. Ingram-Smith, C.; Barber, R.D.; Ferry, J.G. The role of histidines in the acetate kinase from *Methanosarcina thermophila*. *J. Biol. Chem.* **2000**, *275*, 33765–33770. [[CrossRef](#)] [[PubMed](#)]
33. Thibeaux, R.; Weber, C.; Hon, C.C.; Dillies, M.A.; Ave, P.; Coppee, J.Y.; Labruyere, E.; Guillen, N. Identification of the virulence landscape essential for *Entamoeba histolytica* invasion of the human colon. *PLoS Pathog.* **2013**, *9*, e1003824. [[CrossRef](#)] [[PubMed](#)]
34. Ehrenkaufer, G.M.; Haque, R.; Hackney, J.A.; Eichinger, D.J.; Singh, U. Identification of developmentally regulated genes in *Entamoeba histolytica*: Insights into mechanisms of stage conversion in a protozoan parasite. *Cell Microbiol.* **2007**, *9*, 1426–1444. [[CrossRef](#)] [[PubMed](#)]
35. Hon, C.C.; Weber, C.; Sismeiro, O.; Proux, C.; Koutero, M.; Deloger, M.; Das, S.; Agrahari, M.; Dillies, M.A.; Jagla, B.; et al. Quantification of stochastic noise of splicing and polyadenylation in *Entamoeba histolytica*. *Nucleic Acids Res.* **2013**, *41*, 1936–1952. [[CrossRef](#)]
36. Pineda, E.; Vazquez, C.; Encalada, R.; Nozaki, T.; Sato, E.; Hanadate, Y.; Nequiz, M.; Olivos-Garcia, A.; Moreno-Sanchez, R.; Saavedra, E. Roles of acetyl-CoA synthetase (ADP-forming) and acetate kinase (PP_i-forming) in ATP and PP_i supply in *Entamoeba histolytica*. *Biochim. Biophys. Acta* **2016**, *1860*, 1163–1172. [[CrossRef](#)]
37. Vicente, J.B.; Ehrenkaufer, G.M.; Saraiva, L.M.; Teixeira, M.; Singh, U. *Entamoeba histolytica* modulates a complex repertoire of novel genes in response to oxidative and nitrosative stresses: Implications for amebic pathogenesis. *Cell Microbiol.* **2009**, *11*, 51–56. [[CrossRef](#)]
38. Diamond, L.S.; Harlow, D.R.; Cunnick, C.C. A new medium for the axenic cultivation of *Entamoeba histolytica* and other *Entamoeba*. *Trans. R. Soc. Trop. Med. Hyg.* **1978**, *72*, 431–432. [[CrossRef](#)]
39. Strober, W. Trypan blue exclusion test of cell viability. *Curr. Protoc. Immunol.* **2001**, *21*, A.3B.1–A.3B.2. [[CrossRef](#)]
40. Hamann, L.; Nickel, R.; Tannich, E. Transfection and continuous expression of heterologous genes in the protozoan parasite *Entamoeba histolytica*. *Proc. Natl. Acad. Sci. USA* **1995**, *92*, 8975–8979. [[CrossRef](#)]
41. Vines, R.R.; Purdy, J.E.; Ragland, B.D.; Samuelson, J.; Mann, B.J.; Petri, W.A., Jr. Stable episomal transfection of *Entamoeba histolytica*. *Mol. Biochem. Parasitol.* **1995**, *71*, 265–267. [[CrossRef](#)]
42. Koushik, A.B.; Welter, B.H.; Rock, M.L.; Temesvari, L.A. A genomewide overexpression screen identifies genes involved in the phosphatidylinositol 3-kinase pathway in the human protozoan parasite *Entamoeba histolytica*. *Eukaryot. Cell* **2014**, *13*, 401–411. [[CrossRef](#)] [[PubMed](#)]
43. Bradford, M.M. A rapid and sensitive method for the quantitation of microgram quantities of protein utilizing the principle of protein-dye binding. *Anal. Biochem.* **1976**, *72*, 248–254. [[CrossRef](#)]
44. Stoscheck, C.M. Quantitation of protein. *Methods Enzymol.* **1990**, *182*, 50–68. [[PubMed](#)]
45. Neubauer, S.; Chu, D.B.; Marx, H.; Sauer, M.; Hann, S.; Koellensperger, G. LC-MS/MS-based analysis of coenzyme A and short-chain acyl-coenzyme A thioesters. *Anal. Bioanal. Chem.* **2015**, *407*, 6681–6688. [[CrossRef](#)]
46. Rose, I.A.; Grunberg-Manago, M.; Korey, S.R.; Ochoa, S. Enzymatic phosphorylation of acetate. *J. Biol. Chem.* **1954**, *211*, 737–756. [[CrossRef](#)]